

# Conversion electron Mössbauer spectroscopy of the surface crystallization of the $\text{Fe}_{75}\text{Co}_9\text{B}_{16}$ amorphous alloy

T. ZEMČÍK

*Czechoslovak Academy of Sciences, Institute of Physical Metallurgy, Žižkova 22, CS 616 62 Brno, Czechoslovakia*

K. ZÁVĚTA

*Czechoslovak Academy of Sciences, Institute of Physics, Na Slovance 2, CS 180 40 Prague, Czechoslovakia*

I. ŠKORVÁNEK\*

*Slovak Academy of Sciences, Institute of Experimental Physics, Solovjevova 47, CS 043 53 Košice, Czechoslovakia*

Using a new design of helium–methane gas-flow detector of conversion electrons for Mössbauer spectroscopy, non-uniform nucleation of the primary  $\alpha$ -Fe–Co phase on both contact and free surfaces of the  $\text{Ar}(\text{H}_2)$  annealed amorphous  $\text{Fe}_{75}\text{Co}_9\text{B}_{16}$  alloy was observed in its early crystallization stage. In this state the amount of crystalline phase on the contact ribbon side surpasses that on the free one by a factor of three, whereas no traces of volume crystallization were observed in the transmission spectra. By applying ion implantation to both ribbon surfaces, a slight reduction of the crystalline phase contribution was found. Magnetic domain structure observations were performed in order to evaluate the influence of surface crystallization on magnetic properties.

## 1. Introduction

The state of the surface of amorphous ribbons is known to play an important role in the crystallization processes. Conversion electron Mössbauer spectroscopy (CEMS) is one of the renowned methods for studies of the differences between the volume and surface crystallization processes in amorphous alloys (e.g. [1, 2]). By comparing the volume and surface crystallization kinetics and mechanisms, information can be gained on the stability of the amorphous state and of the possible means of its stabilization.

Within the framework of systematic studies of the processes of amorphization, relaxation and crystallization of Fe–Co–B amorphous alloys, the early stages and detection sensitivity of the primary crystallization of  $\alpha$ -Fe–Co solid solution have been investigated. In our previous work [3], the massive occurrence of the surface crystalline phase even in the hypereutectic  $\text{Fe}_{70}\text{Co}_{10}\text{B}_{20}$  amorphous alloy, probably due to boron depletion, was shown.

Until now, a more or less uniform progress of the crystallization on both the free and contact surfaces of amorphous ribbons was reported, though by a closer look at Fig. 1 of Saegnsa and Morrish [4] a somewhat faster onset of crystallization on the dull surface than on the shiny one can be observed. Other authors

[1, 2] have also reported a preference of crystallization start for one of the surfaces. In this work, the effect of a non-uniform nucleation of the metallic  $\alpha$ -Fe–Co phase just at the beginning of the primary crystallization process will be reported as a starting stage in ion implantation experiments.

The influence of ion implantation on the state of the amorphous ribbon surfaces has been a topic of comprehensive studies (e.g. [5]). Implantation was shown to induce changes when magnetization curves were studied by the optical Kerr method by one of the present authors [6]. In the Metglas 2605 Co amorphous alloy he found, for instance, a decrease of the surface coercive field from  $78 \text{ A m}^{-1}$  down to  $22 \text{ A m}^{-1}$  due to the implantation. However, the exact mechanisms of how the implantation influences the magnetic properties still remain unrevealed. Here one of the possible ways, i.e. destruction of the surface crystalline nuclei, will be demonstrated.

## 2. Experimental procedure

Slightly hypoeutectic melt-spun amorphous alloy of nominal composition  $\text{Fe}_{75}\text{Co}_9\text{B}_{16}$  was chosen for the investigations. From a ribbon 6 mm wide and ca.  $25 \mu\text{m}$  thick, samples were made of 10 mm useful

\*Present address: GKSS Forschungszentrum, Max-Planck-Strasse, D-2054 Geesthacht, Germany.

diameter for both transmission and CEMS measurements.

To discern the very beginning of crystallization, the corresponding heat treatment time/temperature were estimated from the isothermal transformation curves and more precisely adjusted by the trial-and-error method: for example, samples annealed at 320 °C/2h gave no traces of crystallization either in the volume or at the surfaces. Finally, annealing at 350 °C for 2 h in purified argon with a slight admixture of H<sub>2</sub> was chosen.

Room-temperature transmission <sup>57</sup>Fe Mössbauer spectra were taken with a computer-controlled double-parabolic drive 500-channel spectrometer using a ca. 1 GBq <sup>57</sup>Co–Cr source and α-Fe calibration of the velocity scale. Similarly, the conversion electron Mössbauer spectra were measured using an improved design of the helium–methane gas-flow detector described elsewhere [7].

All spectra were processed using a flexible matrix-defined FFT-convolution fitting program [8], assuming basic Lorentzian line shapes, possibly broadened by an asymmetric hyperfine induction distribution, modelled by a double-Gaussian function for the amorphous substance superimposed on a Dirac component for the crystalline phase.

The magnetic domain structure was observed by means of a Jeol JXA 733 scanning electron microscope complemented by an auxiliary detector of back-scattered electrons. The oblique incidence of 50 kV primary electron beam gave type II magnetic contrast [9].

Ion implantation was used for structure modification of the surface layers of both as-quenched and annealed (surface-crystallized) amorphous alloys. The implantation was carried out using a Balzers MPB-200 ion accelerator at room temperature in a vacuum of less than 10<sup>-6</sup> torr. The specimens were bombarded by 120 keV accelerated <sup>11</sup>B<sup>+</sup> to a total dose of 5 × 10<sup>15</sup> ions cm<sup>-2</sup>. The implantation process was performed on both sides of the ribbon specimens. The average implantation depth (taken as the maximum of the distribution curve, *R<sub>p</sub>*) was estimated to be approximately 0.15 to 0.20 μm.

### 3. Results

The transmission spectra of both the as-quenched and annealed states are shown in Fig. 1. No traces of any crystalline phase were found by the computer analysis. Similarly, both the contact and free surfaces of the as-quenched ribbon were free of any sign of crystallization as shown in Fig. 2.

On the other hand, CEMS of both sides of the ribbon subjected to the heat treatment reveals clear contributions of the crystalline nuclei. This can be seen in Fig. 3, in which the hyperfine induction distribution functions consisting of the Gaussian and Dirac contributions corresponding to the amorphous and crystalline phases, respectively, are also plotted. The same picture for the implanted sample is shown in Fig. 4.

From the quantitative numerical results yielded by the fitting program, average hyperfine inductions for

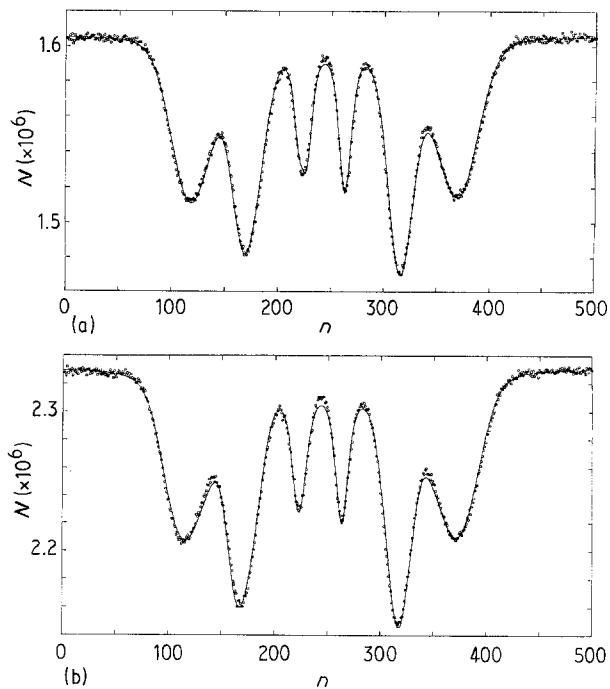


Figure 1 Transmission Mössbauer spectra of samples (a) as quenched and (b) annealed 350 °C/2 h; *n* = channel No., *N* = number of counts, (—) least-squares fit.

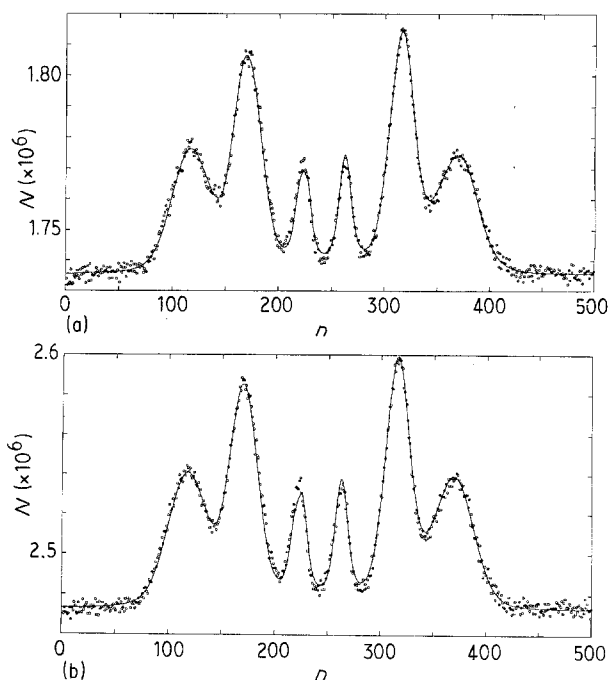


Figure 2 Conversion electron Mössbauer spectra of (a) free and (b) contact surfaces of as-quenched Fe<sub>75</sub>Co<sub>9</sub>B<sub>16</sub> amorphous alloy; *n* = channel No., *N* = number of counts, (—) least-squares fit.

both the detected amorphous and crystalline phases along with the corresponding relative areas of their spectral contributions are collected in Table I.

The effect of ion implantation is seen to be negative for the as-quenched and pre-crystallization-annealed samples, where consistently no crystalline nuclei were found at their surfaces. On the other hand, due to the implantation effects, the amount of crystalline phase on both the free and contact surfaces of the surface-crystallized ribbons is approximately uniformly diminished.

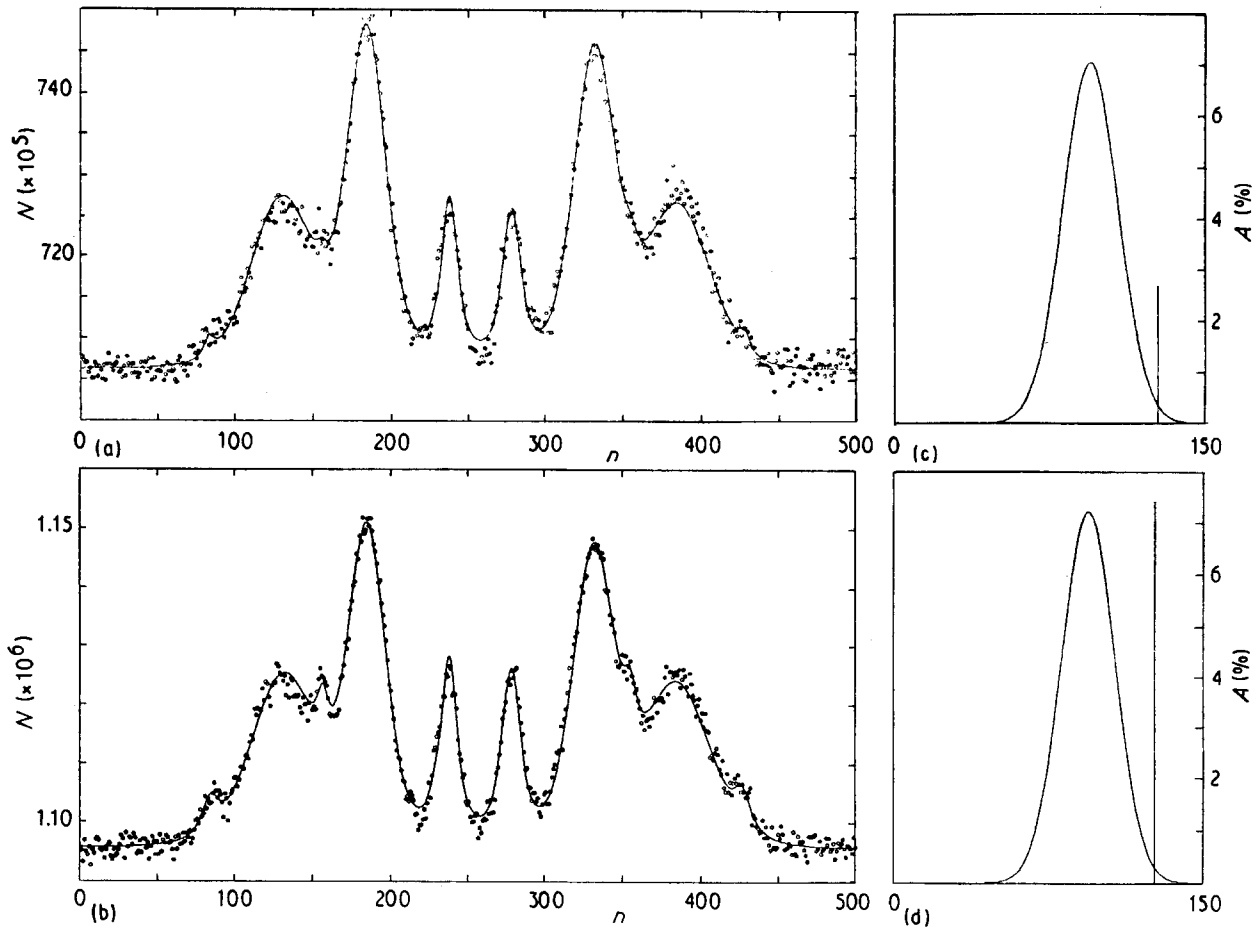


Figure 3 Conversion electron Mössbauer spectra of (a) free and (b) contact surfaces of annealed ( $350^{\circ}\text{C}/2\text{ h}$ ) amorphous alloy, along with (c, d) the corresponding hyperfine inductions distributions;  $n$  = channel No.,  $N$  = number of counts,  $A$  = relative area in the  $P(B)$  distribution, (—) least-squares fit.

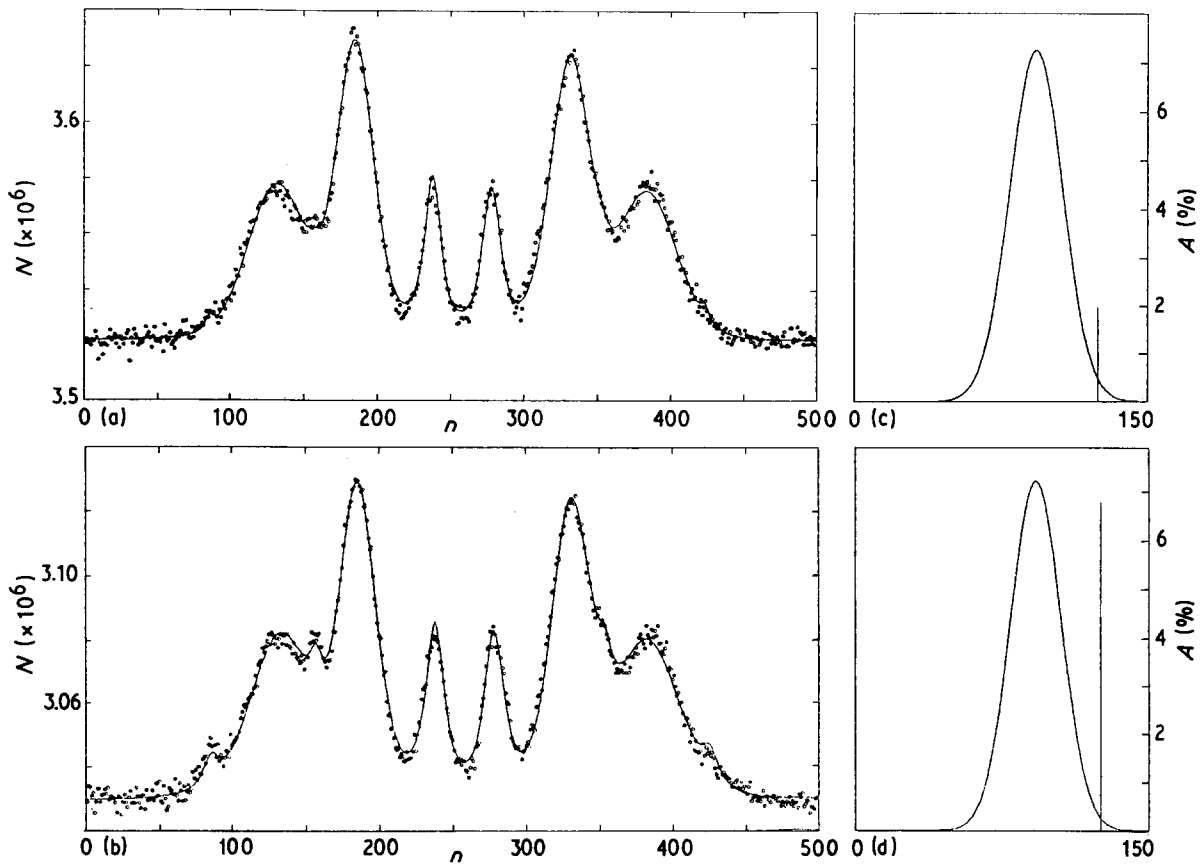


Figure 4 Conversion electron Mössbauer spectra of (a) free and (b) contact surfaces of annealed ( $350^{\circ}\text{C}/2\text{ h}$ ) and  $^{11}\text{B}^+$  implanted amorphous alloy, along with (c, d) the corresponding hyperfine inductions distributions;  $n$  = channel No.,  $N$  = number of counts,  $A$  = relative area in the  $P(B)$  distribution, (—) least-squares fit.

TABLE I Hyperfine inductions,  $B$ , and relative areas,  $A$ , of the amorphous and crystalline Fe-Co(-B) phases

State	Side	$B_{am}(T)$	$\Delta B_{am}(T)$	$B_{cr}(T)$	$A_{cr}(\%)$
As-quenched	Volume	$25.83 \pm 0.02$	$8.28 \pm 0.06$		0
	Free	$25.81 \pm 0.03$	$7.92 \pm 0.10$		0
	Contact	$25.76 \pm 0.03$	$7.75 \pm 0.10$		0
As-quenched + implanted	Free	$25.95 \pm 0.04$	$8.00 \pm 0.13$		0
	Contact	$25.92 \pm 0.04$	$8.24 \pm 0.16$		0
Annealed 350°C/2 h	Volume	$26.23 \pm 0.02$	$8.36 \pm 0.06$		0
	Free	$26.24 \pm 0.04$	$8.84 \pm 0.15$	$35.42 \pm 0.07$	$2.7 \pm 0.4$
	Contact	$26.11 \pm 0.04$	$8.52 \pm 0.13$	$35.21 \pm 0.08$	$7.3 \pm 0.4$
Annealed + implanted	Free	$26.04 \pm 0.03$	$8.85 \pm 0.12$	$34.77 \pm 0.16$	$1.9 \pm 0.3$
	Contact	$25.83 \pm 0.04$	$8.41 \pm 0.13$	$35.02 \pm 0.09$	$6.8 \pm 0.4$

The changes in domain structure were observed on ca. 10 mm long pieces of the ribbons. The directions of local easy axes were almost randomly distributed. The as-received sample showed large changes of domain width upon application of an external magnetic field of about  $1 \text{ A cm}^{-1}$ , whereas the domain structure of heat-treated samples was already sensitive, at least in some regions, to fields of  $0.3 \text{ A cm}^{-1}$ . The behaviour of stress-relieved and partly crystallized samples was rather similar, the only difference being in the higher value of remanence for the latter one.

#### 4. Discussion

It follows from Figs 1 and 2, and quantitatively from Table I, that no traces of crystallization were observed in the as-quenched state and in the volume of the annealed sample. The average hyperfine magnetic inductions in the bulk and at both surfaces of the as-quenched state match well together, not revealing any differences in composition and/or structure between them as well as no deviation from the amorphous structure.

The same holds for the amorphous contributions in the annealed state, with maybe a slightly higher induction in the bulk indicating some surface composition changes. What is to be noticed is pronouncedly higher values of these inductions as a result of annealing. This increment of about 2% agrees well with our previous results [10] reporting a systematic hyperfine induction increase as a result of various relaxation processes in the amorphous state.

The most remarkable feature of the CEMS spectra of both surfaces in the annealed state is the presence of a weak sextet with a large splitting and narrow lines belonging to the surface crystalline nuclei (Fig. 3). Their hyperfine inductions as listed in Table I surpass the value of 33 T for pure  $\alpha$ -iron, thus indicating their alloying with cobalt.

In contrast to the previously reported surface crystallization observations using the CEMS method [1–3], the nucleation is strongly non-uniform, favouring by a factor of three (Table I) the contact side of the amorphous ribbon. Substantially the same situation remains at both surfaces of the implanted samples (Table I) where a remarkable decrease of the crystalline phase contents is observed, indicating cer-

tain re-amorphization of the surfaces due to the implantation process.

Taking into account the above increase of the average hyperfine induction of amorphous alloys due to irreversible relaxation processes, it is interesting to observe the  $B_{am}$  changes in Table I as a consequence of the implantation: both annealing and implantation increase the induction of the amorphous phase in the as-quenched state, hence acting as relaxation factors, whereas the implantation causes an induction decrease of the annealed state, obviously playing the above mentioned re-amorphization role.

Closer comparison of the widths of the hyperfine induction distributions at the free and contact surfaces (cf. Figs 3 and 4) reveals the reversal or enhancement of their difference, favouring the former one to be somewhat broader (Table I). This may be caused [3] by changes in the chemical composition due to segregation phenomena between the crystallites and the amorphous remainder.

#### Acknowledgements

Thanks are due to Dr N. A. Tomashevskii, Institute of Metal Physics, Ukrainian Academy of Sciences, Kiev, for kindly providing the master alloy and to Ing. P. Duhaj, Physical Institute, Centre of Electro-Physical Research, Slovak Academy of Sciences, Bratislava, Czechoslovakia, for preparation of the amorphous ribbon.

#### References

1. H.-G. WAGNER, M. ACKERMANN, R. GAA and U. GONSER, in Proceedings, 5th International Conference on Rapidly Quenched Metals, RQM 85, Vol. 1, Edited by S. Steeb and H. Warlimont (Amsterdam, 1985) p. 247.
2. M. ACKERMANN, H.-G. WAGNER, U. GONSER and P. SKINER, *Hyperf. Int.* **27** (1986) 397.
3. J. PAVLOVSKÝ and T. ZEMČÍK, *Phys Status Solidi (a)* **112** (1989) K1.
4. N. SAEGUSA and A. H. MORRISH: *Phys. Rev.* **B26** (1982) 6547.
5. G. SEFÖZÖ, L. F. KISS, Cs. D. DARÓCZI, É. KISDI-KOSZÓ and G. VÉRTESY, *IEEE Trans. Magn.* **26** (1991) 1418.
6. I. ŠKORVÁNEK and P. KOLLÁR, to be published.
7. N. TOMASHEVSKII, S. HAVLÍČEK, Yu. GALUSHKO and T. ZEMČÍK, *Nucl. Instr. Meth.* submitted.

8. V. VESELÝ and T. ZEMČÍK, in Proceedings of International Conference on Applications of the Mössbauer Effect, ICAME 89, Budapest, 1989, *Hyperf. Int.* **58** (1990) 2679.
9. K. ZÁVĚTA, K. JUREK, P. DUHAJ, *Czech. J. Phys.* **B37** (1987) 42.
10. T. ZEMČÍK, in Proceedings of International Conference on

Applications of the Mössbauer Effect, ICAME 89, Budapest 1989, *Hyperf. Int.* **55** (1990) 1099.

*Received 26 July 1991  
and accepted 11 March 1992*